Molecular Dynamics Simulations of Angiotensin II in Aqueous and Dimethyl Sulfoxide Environments

Marco A. C. Preto,[†] André Melo,[†] Hernâni L. S. Maia,[‡] Thomas Mavromoustakos,[§] and Maria J. Ramos*,[†]

REQUIMTE, Departamento de Química, Faculdade de Ciências, Universidade do Porto, Rua do Campo Alegre, 687, 4169−007 Porto, Portugal, Departamento de Química, Universidade do Minho, Gualtar, 4710-057 Braga, Portugal, and Institute of Organic and Pharmaceutical Chemistry, National Hellenic Research Foundation, Vas. Constantinou 48, 11635, Athens

Received: April 22, 2005; In Final Form: July 8, 2005

Angiotensin II (Ang II) is an octapeptidic hormone, which plays an important role in the mechanisms of blood pressure control. In this work, extensive molecular dynamics (MD) simulations have been carried out on this peptide, both in aqueous and in dimethyl sulfoxide (DMSO) environments. Experimentally proposed models for the structure of angiotensin II in both environments are not consensual and the results obtained have provided some further insight about the structural properties of this hormone. In these simulations, the N-terminus of Ang II in the aqueous environment has been associated with a considerable larger flexibility than the correspondent C-terminus, but this was not found in the case of the DMSO environment. This is consistent with the assumption that the biological activity of Ang II is associated with its C-terminal residues embedded in a hydrophobic environment of its AT1 receptor. Other features detected in DMSO environment were an H(His6 imidazole)−O(Phe8 carboxylate) hydrogen bond and a salt-bridge structure involving the Asp1 and Arg2 side chains. An additional important conformational feature is the spatial proximity between Tyr4 and His6 in both water and DMSO environments. This molecular feature may trigger the interest for the synthetic chemists to apply rational design for the synthesis of novel AT1 antagonists.

Introduction

Hypertension is one of the most common health problems in the developed countries and several different clinical approaches have been used to prevent this chronic disease.[1] The renin−angiotensin−aldosterone system (RAAS) is one of the most important regulators of blood pressure and it plays a central role in the expression and modulation of cardiovascular diseases.[1] Angiotensin II (Ang II), an octapeptidic hormone (Asp1-Arg2-Val3-Tyr4-Ile5-His6-Pro7-Phe8), is the primary active agent of the RAAS system. Ang II exerts most of its biological functions by activating angiotensin type 1 (AT1) receptors. Blood hypertension is usually related to excess production of this hormone, and the most successful antihypertensive drugs, to date, prevent the formation of this hormone or antagonize its interaction with the AT1 receptor.[2]

The most important features for agonist and antagonist activities have been identified by structure−activity studies.[3−5] Significant evidences point to the fact that polar and charged residues of Ang II such as Arg2, Tyr4, and His6 together with the terminal carboxylate are crucial for binding to the AT1 receptor, whereas the Tyr4, His6, and Phe8 together with its carboxylate are essential for activation of this receptor. A common conformational feature for Ang II and its peptide analogues has been proposed from both NMR in DMSO and molecular modeling techniques to simulate the AT1 receptor environment.[4−10] A backbone turn located between residues 2 and 5, has been found in this hormone, in its agonists and in its type 1 noncompetitive antagonists.[4] Additionally, the Phe8 terminal residue induces strong conformational restrictions for both Ang II and its agonist analogues, whereas the C-terminus of type I antagonists containing an aliphatic residue at position 8 presents much more flexibility.[4−9] These results have supported the hypothesis of a common mode for binding the N-terminus of Ang II and its analogues with the AT1 receptor.[4] It has been suggested also that the presence of a cluster of side chain aromatic rings involving the triad of amino acids (Tyr4, His6, and Phe8) promotes an appropriate C-terminus conformation for receptor activation by both Ang II and its agonists, whereas the conformational flexibility of C-terminus of type I antagonists is considerably less favorable for this purpose.[4−9] However, other NMR[10] and mutagenesis[11] studies excluded the existence of this cluster, inferring that the Phe8 side chain is too far apart from the His6 and Tyr4 aromatic rings. This work reports a systematic MD study of this octapeptide in both aqueous and DMSO environments, which provides further insight into the Ang II structure and its dependence on the surrounding environment. Such theoretical work may enhance the validity of certain experimental models reported in the literature using different physicochemical methods and experimental conditions as well as to trigger the synthetic interest for novel antihypertensive analogues.

Simulation Details

System Setup. The conformational behavior of Ang II was simulated in aqueous and in DMSO solutions. For both

* Corresponding author. E-mail: mjramos@fc.up.pt.
[†] Universidade do Porto.
[‡] Universidade do Minho.
[§] National Hellenic Research Foundation.

10.1021/jp0521048 CCC: $30.25
Published on Web 08/26/2005

simulations, the starting geometry of Ang II was obtained in DMSO solution using NMR techniques by Matsoukas and coworkers.[6]

This structure was placed in preequilibrated solvent boxes. The aqueous system contained initially 3260 TIP3P water molecules,[12] whose relative orientation was obtained from the Amber 6 package,[13] in a 50.985 Å cubic box. The DMSO system had initially 772 OPLS DMSO molecules,[14] whose initial orientation was obtained from the PACKMOL package,[15] in a 48.73 Å cubic box. This system was subsequently equilibrated in an isobaric−isothermal ensemble (*NPT*) for 1 ns at 300 K and 1 atm, using the Berendsen thermostat and barostat[16] with coupling constants of 1.0 and 0.2 ps, respectively. For both systems, the overlapping solvent molecules were deleted when the distance between one of their atoms and any solute atom was lower than the sum of the correspondent VdW radii. An additional molecular dynamics simulation of Ang II in a vacuum was carried out during 2.0 ns at 300 K, to evaluate the importance of the intramolecular interactions in a solvent free environment. In all these simulations, Ang II was described by the AMBER force field.[17−19]

Molecular Dynamics Simulations. The initial structures were minimized, keeping the solute fixed, until the root-mean-square energy gradients were lower than 0.0001 kcal mol^{-1}. About 20000 steps were used, with the first 2000 steps performed using the steepest descent method and the remaining steps carried out using the conjugate gradient method. The systems simulated in solution were initially heated using a temperature gradient from 0 to 300 K for 50 ps in a canonical (*NVT*) ensemble, using the Berendsen temperature coupling method[16] with a coupling constant of 1.0 ps. These systems were then equilibrated, first in an *NVT* ensemble and subsequently in an isobaric−isothermal (*NPT*) ensemble. The equilibration times were 50 ps in the *NVT* ensemble for both systems. These were followed by simulations in the *NPT* ensemble (equilibration and production) with a total duration of 2 ns for the aqueous system and 5 ns for the system using DMSO as solvent. These *NPT* ensemble simulations were carried out at 300 K and 1 atm, using the Berendsen thermostat and barostat,[16] with coupling constants of 1.0 and 0.2 ps, respectively. These simulations were performed using periodic boundary conditions. The equations of motion were integrated every 1 fs using the Verlet leapfrog algorithm[20] and SHAKE constrains[21] were applied to all bonds linking hydrogen and heavy atoms. The partical mesh Ewald (PME) method[22,23] was used to evaluate the long-range electrostatic interactions and a continuum model was used for the estimation of VdW long-range interactions. A distance cutoff of 12 Å (with a skin value of 2 Å) was used to generate the list of nonbond pairs, which was updated whenever any atom had moved more than 1 Å since the last list update. Structural and thermodynamic properties were stored every 50 steps (0.050 ps) for analysis. All simulations were carried out in a dual Pentium IV Xeon computer, using the Amber 6 package.[13] The 3D structure images presented wherein were created with VMD.[24]

Results and Discussion

To provide a quantitative characterization of the Ang II behavior in both solvation environments simulated in this work, a set of structural parameters was monitored as a function of simulation time. These parameters provide a general idea of the folding and structural behavior of Ang II, and allow us to test several features proposed experimentally. These were the following:

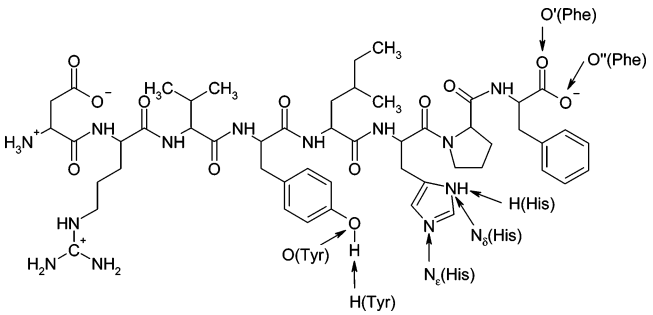

Figure 1. Structural formula of angiotensin II. The arrows indicate relevant atoms for the discussion presented in this work.

- all Φ and Ψ dihedral angles of the backbone chain;
- the distance between the C_α of residue *i* and the C_α of residue *i*+3;
- the angle involving O(Tyr)−H(Tyr)−N(His) (see Figure 1);
- the angle involving N_δ(His)−H(His)−O′(Phe) or −O″(Phe) (see Figure 1);
- the angle between the planes formed by the Tyr4 and the His6 side chain rings;
- the angle between the planes formed by the His6 side chain ring and the Phe8 carboxylate group;
- the distance between the H(Tyr) and the N_ϵ(His) (see Figure 1);
- the distance between the H(His) and the oxygen atoms in the terminal carboxyl group (see Figure 1).

To simplify the systematization of the backbone orientation of each residue, their Φ and Ψ dihedral angles were first represented as a function of simulation time. From the collected data, the marginal (for each dihedral angle) and joint (Φ vs Ψ) probabilities were evaluated. Typical results, obtained for Arg2, are presented as an example in Figure 2. The local backbone conformers for each residue are presented in Table 1. A statistical analysis of the conformational behavior of Ang II backbone has demonstrated that these local conformers can be considered independently. Therefore, the global backbone conformers can be obtained from all possible combinations of the local conformers. In both simulations, the backbone dihedrals assumed fairly well-defined structures. The simulation in DMSO revealed a total of four main backbone conformers (with two of them being dominant during over 85 % of the simulation time). Ang II presented considerable larger flexibility in aqueous environment. In fact, 16 main backbone conformers were identified in the simulation carried out in this environment. The C-terminus of Ang II, from residue Tyr4 to residue Phe8, was particularly well conserved in both simulations. The correspondent N-terminus, from residue Asp1 to residue Tyr4, was observed to be much more flexible and responsible for almost all the conformational variability observed. At the other end, Ang II adopts a very well preserved folded structure in a vacuum with all charged groups in close contact. To provide an appropriate visualization of the conformational space occupied by the Ang II backbone, its more rigid C-terminus (from atom C_α of Tyr4 to atom N of Phe8) is used to superimpose the different conformers obtained by MD simulations. The results obtained, presented in Figure 3, illustrate that the conformational variability of Ang II is strongly favored by the hydrophilicity of the environment (vacuum < DMSO < water).

The conformational preference of the bioactive C-terminus was analyzed in detail. Accordingly the geometrical parameters associated with a possible formation of the conjugated Tyr4 hydroxyl−His6 imidazole−Phe8 carboxylate hydrogen bonds were monitored as a function of simulation time. This includes

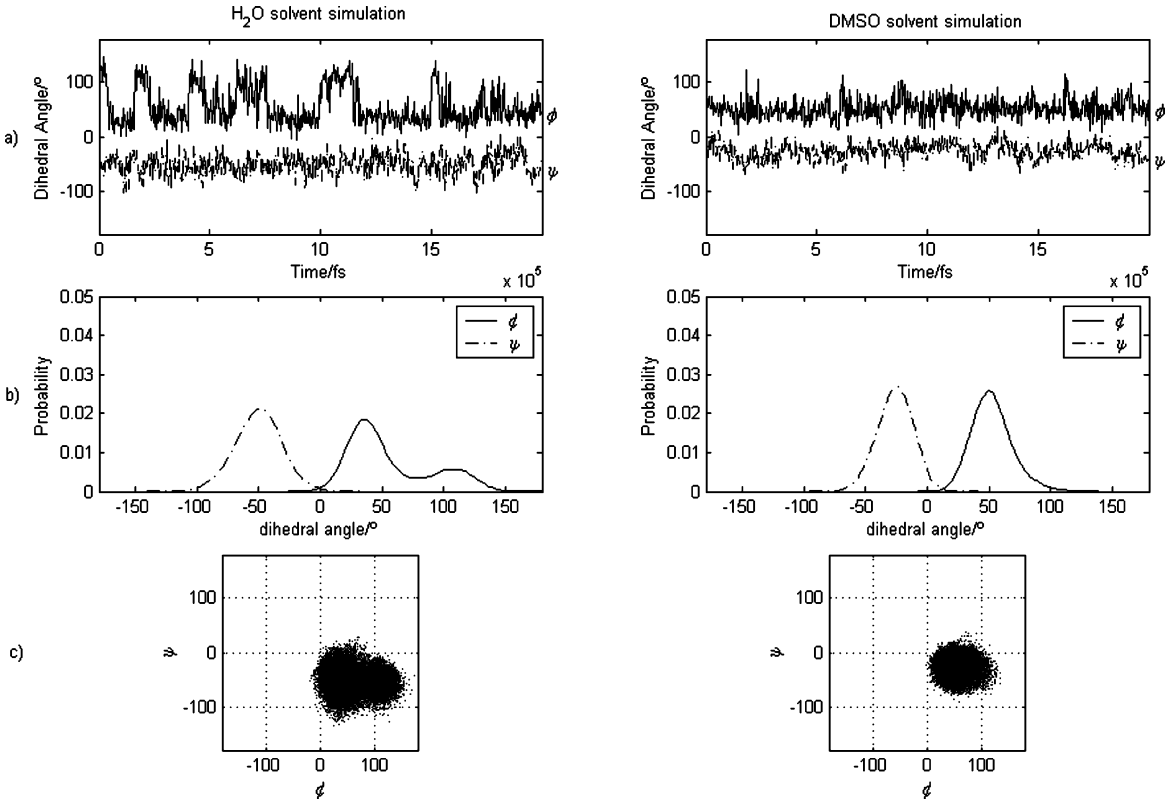

Figure 2. Conformational behavior of backbone Arg2 dihedral angles obtained by molecular dynamics simulations: (a) evolution of dihedral angles as a function of simulation time; (b) marginal probabilities plots; (c) joint Φ vs Ψ probability plots.

TABLE 1: Local and Global Backbone Conformers of Angiotensin II, Obtained by Molecular Dynamics Simulations[a]

	simulation in water		simulation in DMSO	
residue	no. of conformers	characterization[b]	no. of conformers	characterization[b]
Asp1	3	($\varphi \approx 60$; $\psi \approx 40$); ($\varphi \approx -60$; $\psi \approx 40$); ($\varphi \approx 180$; $\psi \approx 40$)	3	($\varphi \approx 55$; $\psi \approx 30$); ($\varphi \approx 180$; $\psi \approx 30$); ($\varphi \approx -65$; $\psi \approx 30$)1
Arg2	2	($\varphi \approx 35$; $\psi \approx -50$); ($\varphi \approx 105$; $\psi \approx -50$)	1	($\varphi \approx 50$; $\psi \approx -28$)
Val3	4	($\varphi \approx 50$; $\psi \approx -55$); ($\varphi \approx 105$; $\psi \approx -55$); ($\varphi \approx 50$; $\psi \approx -35$); ($\varphi \approx 105$; $\psi \approx -35$)	2	($\varphi \approx 110$; $\psi \approx -30$); ($\varphi \approx 50$; $\psi \approx -30$)
Tyr4	2	($\varphi \approx 35$; $\psi \approx -45$); ($\varphi \approx 105$; $\psi \approx -45$)	1	($\varphi \approx 100$; $\psi \approx -55$)
Ile5	1	($\varphi \approx 40$; $\psi \approx -35$)	1	($\varphi \approx 98$; $\psi \approx -60$)
His6	1	($\varphi \approx 115$; $\psi \approx -35$)	2	($\varphi \approx 30$; $\psi \approx -28$); ($\varphi \approx 100$; $\psi \approx -28$)
Pro7	1	($\varphi \approx 115$; $\psi \approx 130$)	1	($\varphi \approx 105$; $\psi \approx 145$)
Phe8	2	($\varphi \approx 40$; $\psi \approx 125$); ($\varphi \approx 40$; $\psi \approx -30$)	1	($\varphi \approx 30$; $\psi \approx -35$)
Ang II	16		4	

[a] The Φ and Ψ dihedral angles are presented in degrees. [b] The local backbone conformers were demonstrated to be reasonably independent. Therefore, the global backbone conformers were obtained from all possible combinations of the local conformers (excluding the terminal dihedrals due to their intrinsic freedom).

TABLE 2: Distances between $C_\alpha i$ and $C_\alpha i+3$ (in Å)

	simulation in water			simulation in DMSO		
	av	max	min	av	max	min
C_α1(Asp)−C_α4(Tyr)	10.0078	11.3208	7.7010	10.2318	11.3169	8.2686
C_α2(Arg)−C_α5(Ile)	9.8850	11.2097	7.6960	9.1175	10.4600	7.3395
C_α3(Val)−C_α6(His)	10.4002	11.3363	8.7628	9.3006	10.8958	7.5932
C_α4(Tyr)−C_α7(Pro)	9.6078	11.2372	7.7459	10.1537	11.2377	8.3984
C_α5(Ile)−C_α8(Phe)	8.9494	10.3290	7.1238	9.2719	10.0543	8.1402

two distances (H(Tyr4)−N_ϵ(His6) and H(His6)−O(Phe8)), two bond angles (O(Tyr4)−H(Tyr4)−N_ϵ(His6) and N_δ(His6)−H(His6)−O(Phe8)) and two inter-planar angles (one between Tyr4 and His6 side chain rings and other between His6 side chain ring and the Phe8 carboxylate plane).

The optimal parameters for the formation of a hydrogen bond are an interatomic distance between 1.6 and 2.4 Å (average rdf in water is between 1.8 and 1.9 Å), a bond angle (atom 1−H- - - atom 2) as near as possible to 180° and an appropriate orientation of the interplanar angles. This orientation must optimize the orientation of the electronegative atom's electronic density toward the bridging hydrogen.

In the performed simulations, the existence of a hydrogen bond between H(Tyr) and N_ϵ(His) could not be confirmed. In fact, the correspondent distances were usually too large and the angular orientations were not appropriate to establish this bond (see Table 3 and Figures 4−7). On the other hand, the hydrogen bond between H(His) and O′(Phe) (or O″(Phe)) was very well

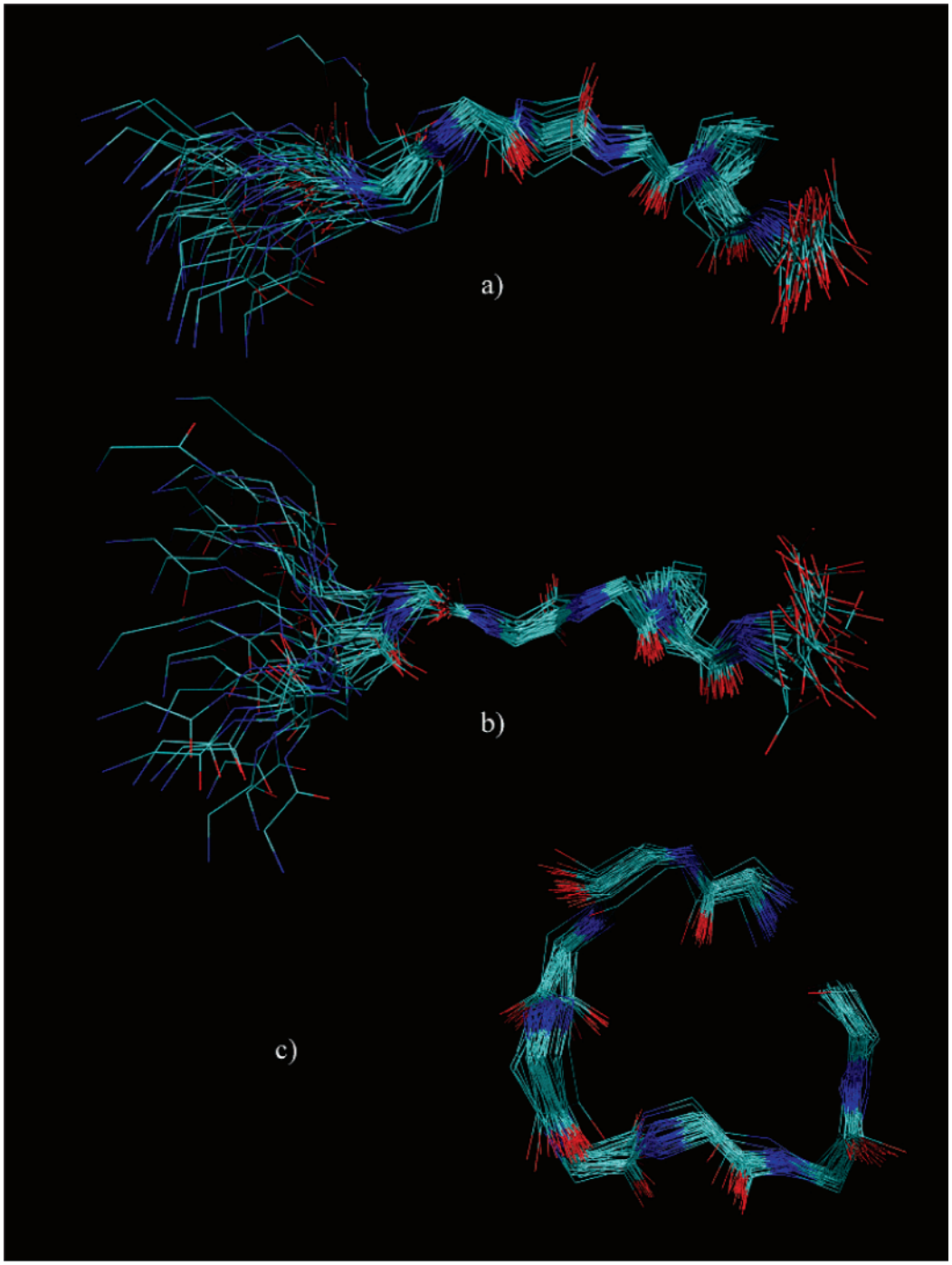

Figure 3. Superimposition of backbone structures of Angiotensin II, from the simulation performed in DMSO (a), aqueous environments (b), and vacuum (c). The frames were collected at 50 ps intervals, and the C-terminal residues heavy atoms were chosen as the fitting points of the superimposition. It can be observed that the backbone conformational variability increases with the hydrophilicity of the environment and from the C-terminus to the N-terminus.

TABLE 3: Relevant Side Chain Distances (in Å) and Angles (in deg)

	simulation in water			simulation in DMSO		
	av	max	min	av	max	min
angle O(Tyr)−H(Tyr)−N_ϵ(His)	59.7621	179.6232	0.2259	92.9531	151.0961	0.0826
angle Tyr−His side chain rings	65.8162	89.9990	0.5990	34.6552	89.9960	0.0610
distance H(Tyr)−N_ϵ(His)	6.1732	13.7604	1.7155	8.3434	12.2870	3.8959
angle N_δ(His)−H(His)−O′(Phe)	97.6757	179.7652	4.4663	161.4357	179.8675	116.9124
angle N_δ(His)−H(His)−O″(Phe)	98.2485	179.5053	1.4283	123.9221	178.5932	88.0531
angle His side chain ring−Phe carboxylate	54.5547	89.9990	0.0620	66.9884	90.0000	5.3860
distance H(His)−O′(Phe)	5.6753	10.3364	1.5681	1.8337	3.8540	1.5177
distance H(His)−O″(Phe)	6.0847	11.2364	1.5939	2.9062	4.3748	1.6191

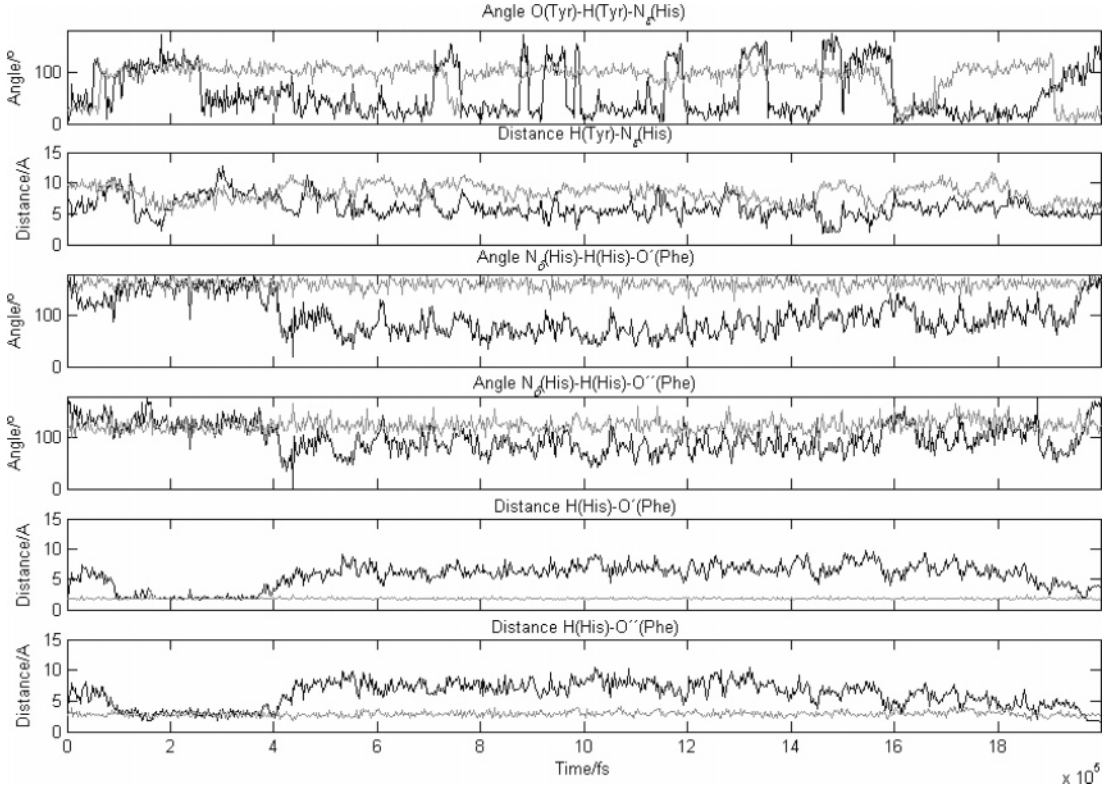

Figure 4. Charts containing the evolution of some selected parameters used. The black lines represent the simulation performed in water and the gray lines represent the DMSO environment simulation. Of particular interest is the data related to the distance H(His)−O′(Phe) and the angle N_δ(His)−H(His)−O′(Phe) of the simulation in DMSO, strongly suggesting the existence of an hydrogen bond, conserved during almost all the simulation.

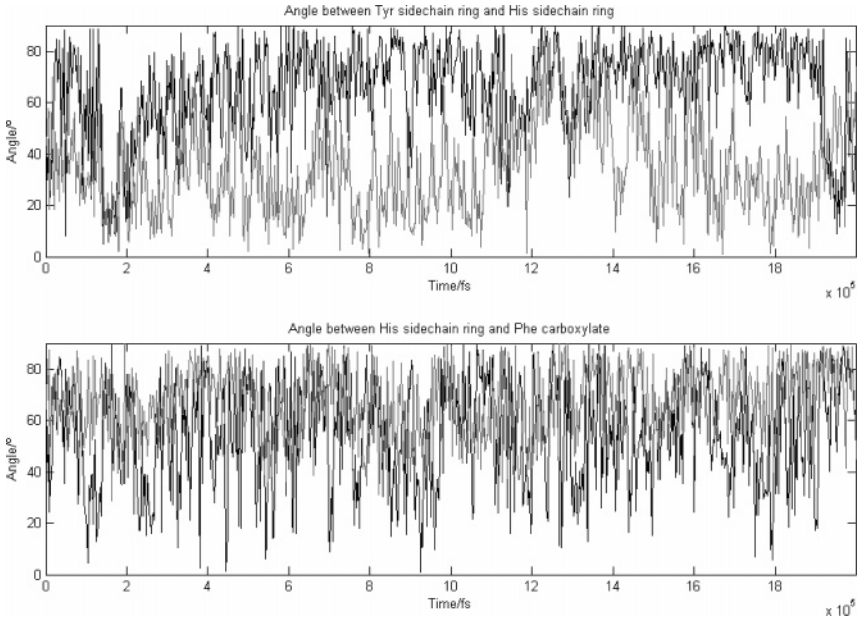

Figure 5. Behavior of the side chain plane angles. The upper graphic refers to tyrosine (residue 4) and histidine (residue 6) side chain rings. The lower graphic pictures the behavior of the angle between the histidine side chain plane and the terminal carboxylate (from residue 8 (phenylalanine)). The black lines represent the simulations in water while the gray lines represent the simulations in DMSO.

conserved during the simulation in DMSO (see Figures 4 and 6 and Table 3). In aqueous environment, this hydrogen bond was only observed in the beginning and the end of the MD simulation (see Figures 4 and 7 and Table 3). This differential behavior is particularly noticeable when comparing Figures 6 and 7, which shows the relative distribution of Tyr4 and Phe8 around the His6 side chain during both simulations. The well-defined arrangement of these residues in DMSO can be seen clearly in Figure 6, as well as the closeness of the atoms involved in the proposed hydrogen bond (between a hydrogen atom of His6 and an oxygen atom of the terminal carboxyl group of Phe8).

Another interesting solvent dependent phenomenon is the relative orientation of Asp1 and Arg2 side chains. In an aqueous environment, both side chains were observed to be well solvated and this effect does not favor their respective association. On the other hand, these same side chains were hardly solvated by DMSO. In this environment, the formations of a salt-bridge

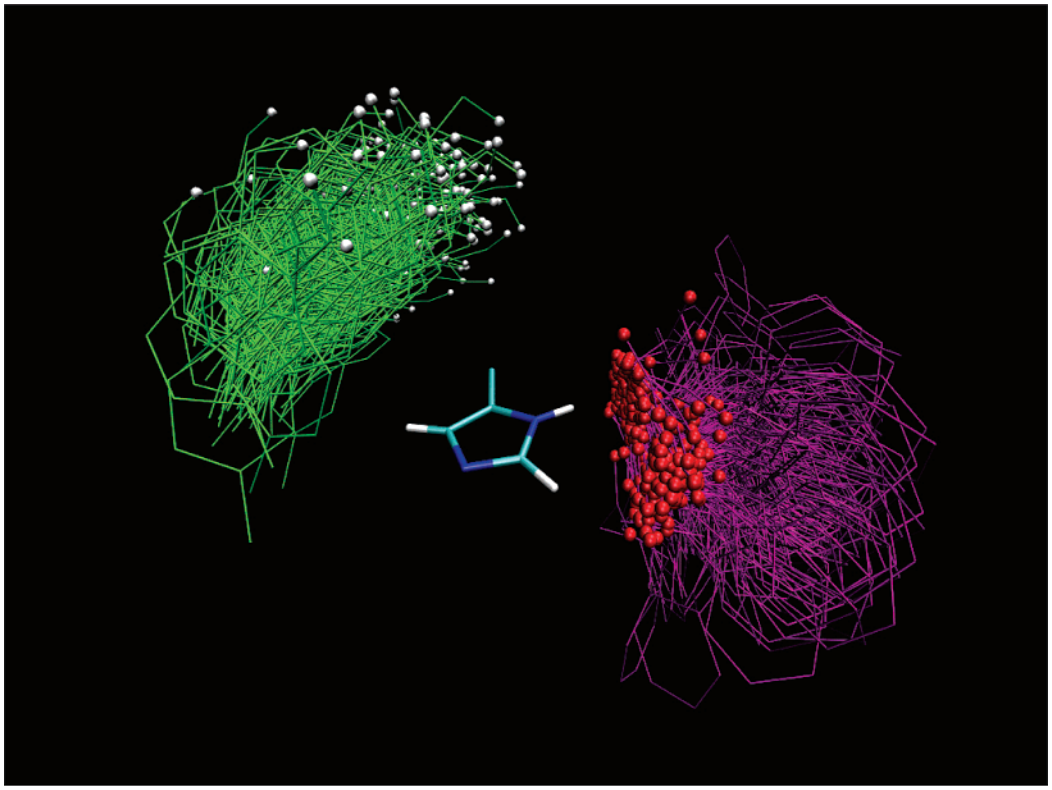

Figure 6. Superimposition of residue 6 side chain (histidine) with projection of the residue 4 side chain (tyrosine, in green) and residue 8 side chain (phenylalanine, in purple) and backbone carbon and oxygen atoms, over the DMSO environment simulation (frames collected at 10 ps intervals). The hydrogen atom of the hydroxyl group of the tyrosine side chain and oxygen atoms of the terminal carboxyl group are represented as spheres for ease of visualization. This figure shows the very well-defined arrangement of these side chains as well as the short distance between the atoms involved in the proposed hydrogen bond (H(His)−O(Phe)).

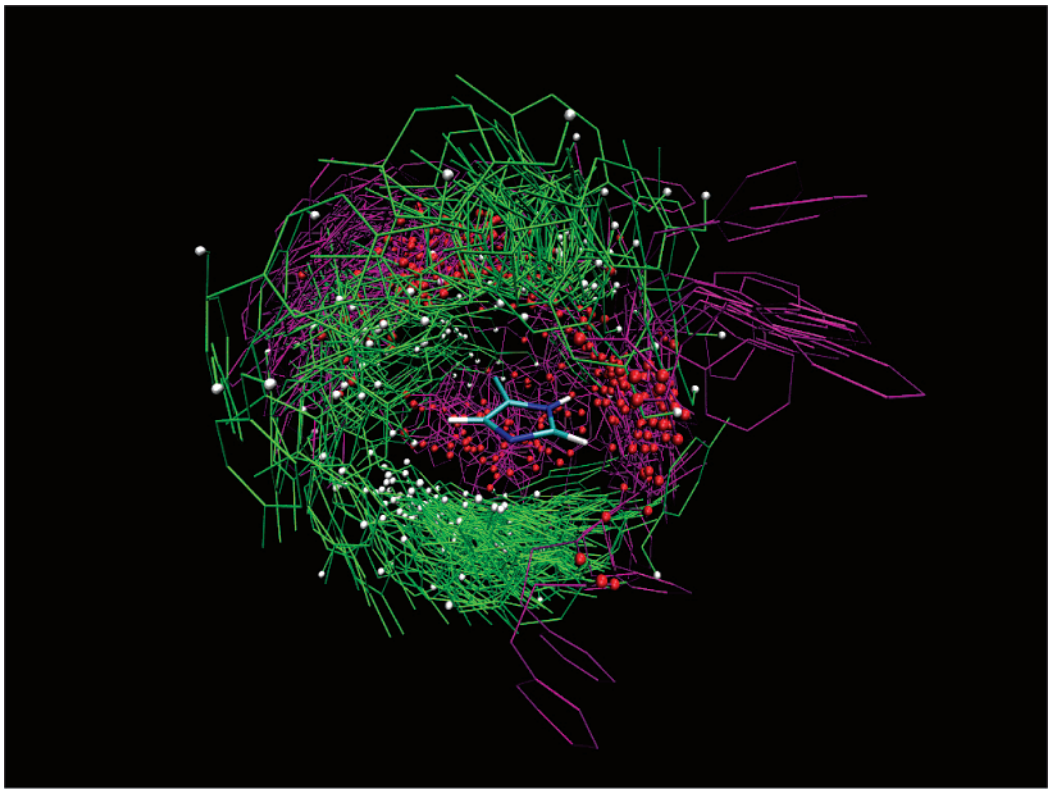

Figure 7. Superimposition of residue 6 side chain (histidine), with projection of the residue 4 side chain (tyrosine, in green) and residue 8 (phenylalanine, in purple) side chain and backbone carbon and oxygen atoms, over the aqueous environment simulation (frames collected at 10 ps intervals). The hydrogen atom of the hydroxyl group of the tyrosine side chain and oxygen atoms of the phenylalanine terminal carboxyl group are represented as spheres for ease of visualization. It can be noticed that the relative dispersion of the tyrosine side chain and the phenylalanine residue are due to the rotation of the histidine side chain ring.

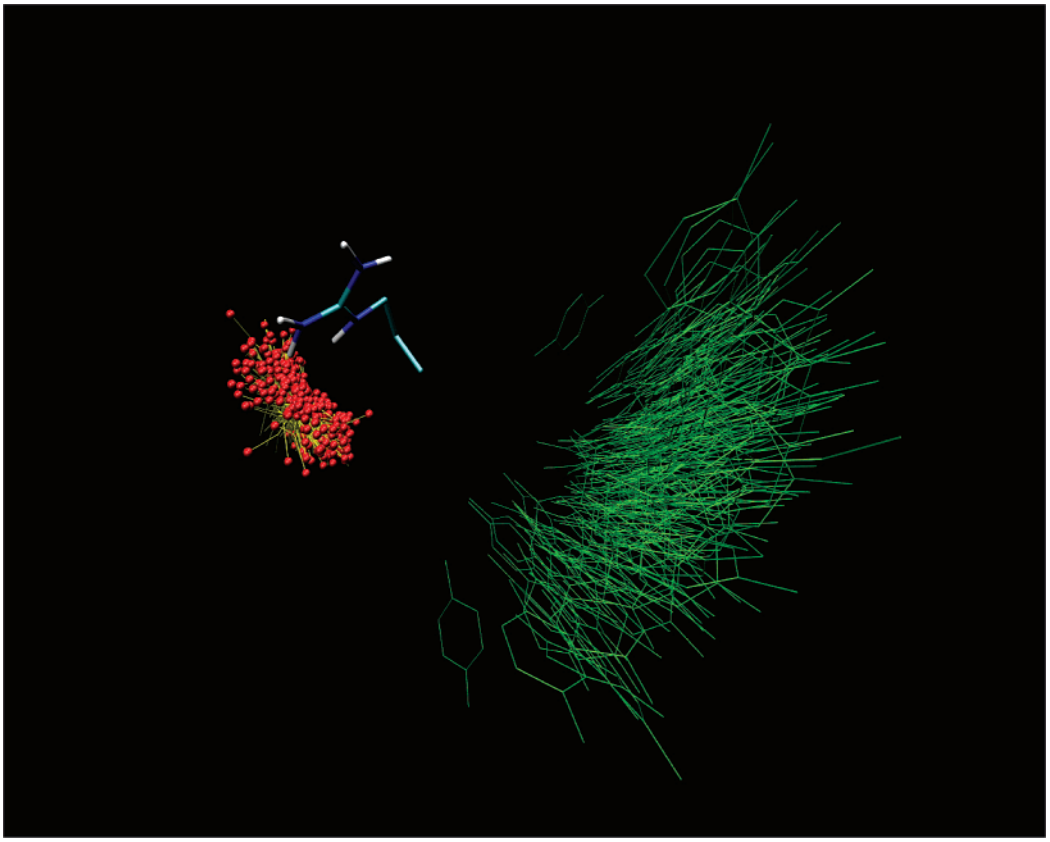

Figure 8. Superimposition of residue 2 side chain (arginine), with projection of the residue 1 (aspartic acid) and residue 4 (tyrosine) side chains over the DMSO environment simulation (frames collected at 10 ps intervals). Note the relative position of the carboxylate and guanidinium groups of the side chains of residues Asp1 and Arg2.

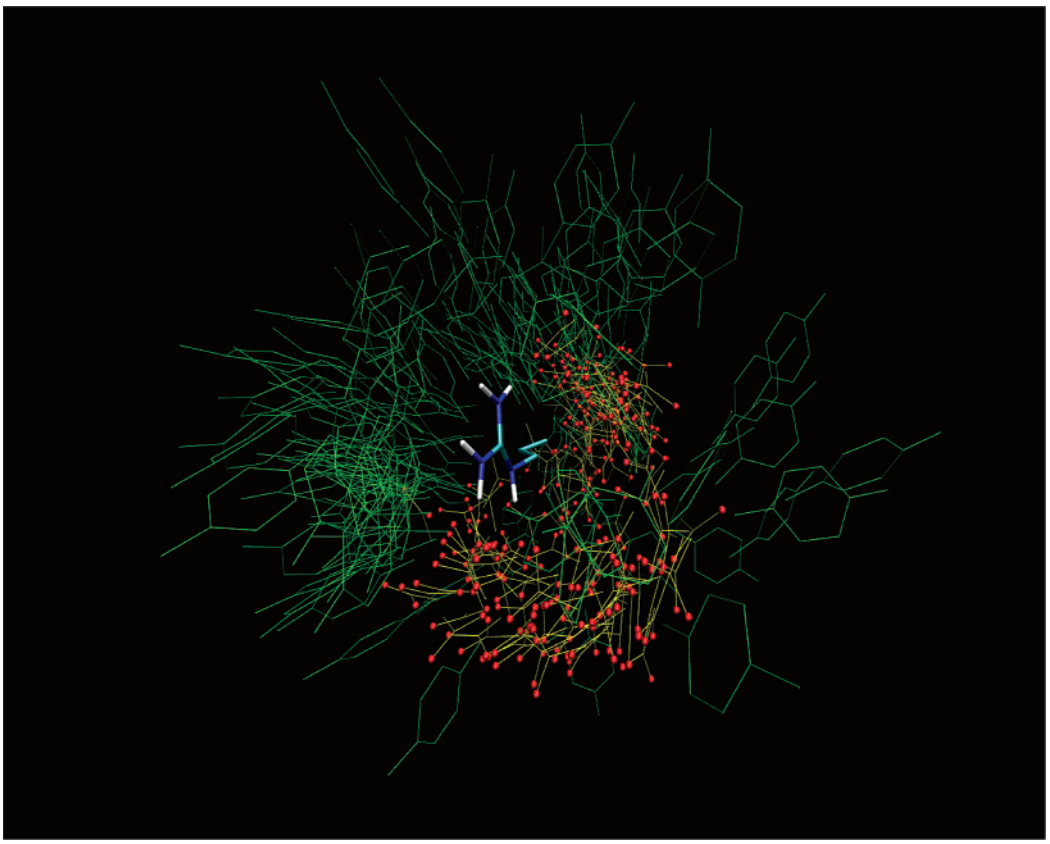

Figure 9. Superimposition of residue 2 side chain (arginine), with projection of the residue 1 (aspartic acid) and residue 4 (tyrosine) side chains over the aqueous environment simulation (frames collected at 10 ps intervals).

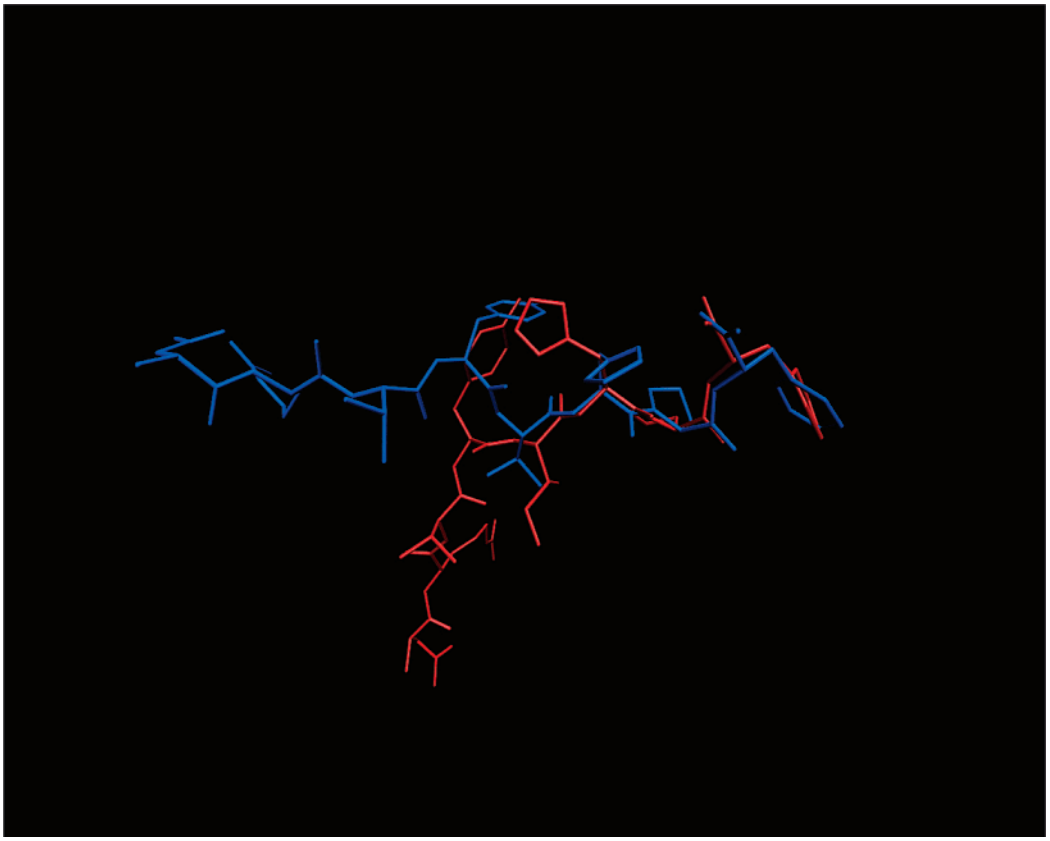

Figure 10. Minimal energy structures found in the simulations. The blue structure corresponds to the simulation performed in DMSO solution and the red structure to the one performed in aqueous environment. We can notice that the C-terminal residues have a very similar structure, even when in a different environment.

structure, stabilized by a strong electrostatic interaction, was very well preserved during the MD simulation. In Figure 8, this association is quite evident, with very short distances between the charged groups of these side chains, whereas in Figure 9, the random spatial disposition of these side chains can be observed.

Conclusions

The active conformation of Ang II has been involved in some degree of controversy,[6,10,11,25−28] with opinions ranging from folded to extended structures. In this work, MD simulations were performed with the objective of eliciting on the conformation of Ang II in both aqueous and DMSO environments.

A very large number of backbone conformers (16) was detected in an aqueous simulation, whereas this peptide presented a much more rigid behavior in DMSO (only 4 backbone conformers were identified). Almost all these conformers were associated with the N-terminus, while the C-terminus was very well conserved. In fact, even in different environments, the C-terminus maintains a similar conformation, which supports its importance to biological activity (see Figure 10).

Some interesting additional features were identified in DMSO solution. This includes an H(His imidazole)−O(Phe carboxylate) hydrogen bond and an Asp1-Arg2 side chain salt-bridge, that were observed to be very well conserved during the MD simulation carried out in this environment. The role of electrostatic intramolecular interactions in the conformation adopted by Ang II is strongly dependent in the hydrophilicity of the environment. In a polar solvent like water, the charged groups are very well solvated and Ang II has a considerable conformational flexibility. The decrease in the solvent polarity favors the electrostatic intramolecular interactions and the more rigid conformations observed in the DMSO simulation. Under the extremely hydrophobic vacuum conditions, all charged groups are in close contact, and Ang II adopts a very well conserved folded structure.

No evidences of the bioactive cluster of aromatic rings (Tyr4-His6-Phe8), suggested by other authors,[4,6,29] were found in our simulations, because the Phe8 side chain was observed to be mainly orientated in the opposite direction of the Tyr4-His6 stacked side chain geometry. Nevertheless, such cluster may occur in a lipid environment or other simulating environment. The proposed conjugated hydrogen bonds do not seem to be compatible with the conformation adopted by this peptide in both simulated environments. In fact, although a His6-Phe8 hydrogen bond has been detected in DMSO simulation, the orientation adopted by the Tyr4 and the His6 side chains was never compatible with the formation of an additional hydrogen bond. However, Tyr4 and His6 side chains were observed to be in close proximity, in agreement with other models derived from experimental data, obtained with different technics.[10,30−33]

The proposed model can be used for synthetic chemists to apply rational design for the synthesis of novel AT1 antagonists. This model can also be considered as a putative for developing novel antihypertensive analogues.

References and Notes

(1) Takahashi, N.; Smithies, O. *Trend. Gen.* **2004**, *20*, 136.

(2) Berl, T. *J. Am. Soc. Nephrol.* **2004**, *15*, S71.

(3) Le, M. T.; Vanderheyden, P. M. L.; Szaszak, M.; Hunyady, L.; Kersemans, V.; Vauquelin, G. *Biochem. Pharm.* **2003**, *65*, 1329.

(4) Wilkes, B. C. Masaro, L.; Schiller, P. W.; Carpenter, K. A. *J. Med. Chem.* **2002**, *45*, 4410.

(5) Matsoukas, J. M.; Polevaya, L.; Ancans, J.; Mavromoustakos, T.; Kolocouris, A.; Roumelioti, P.; Vlahakos, D. V.; Yamdagni, R.; Wu, Q.; Moore, G. J. *Biorg. Med. Chem.* **2000**, *8*, 1.

(6) Matsoukas, J.; Hondrelis, J.; Keramida, M.; Mavromoustakos, T.; Makriyanni, A.; Yamdagni, R.; Wu, Q.; Moore, G. J. *J. Biol. Chem.* **1994**, *269*, 5303.

(7) Roumelioti, P.; Tselios, T.; Alexopoulos, K.; Mavromoustakos, T.; Kolocouris, A.; Moore, G. J.; Matsoukas, J. *Biorg. Med. Chem. Lett.* **2000**, *10*, 755.

(8) Roumelioti, P.; Polevaya, L.; Zoumpoulakis, P.; Giatas, N.; Mutule, I.; Keivish, T.; Zoga, A.; Vlahakos, D.; Iliodromitis, E.; Kremastinos, D.; Grdadolnik, S. G.; Mavromoustakos, T.; Matsoukas, J. *Biorg. Med. Chem. Lett.* **2002**, *12*, 2627.

(9) Polevaya, L.; Mavromoustakos, T.; Zoumpoulakis, P.; Grdadolnik, S. G.; Roumelioti, P.; Giatas, N.; Mutule, I.; Keivish, T.; Vlahakos, D. V.; Iliodromitis, E. K.; Kremastinos, D. Ph.; Matsoukas, J. *Biorg. Med. Chem.* **2001**, *9*, 1639.

(10) Spyroulias, G. A.; Nikolakopoulou, P.; Tzakos, A.; Gerothanassis, I. P.; Magafa, V.; Manessi-Zoupa, E.; Cordopatis, P. *Eur. J. Biochem.* **2003**, *270*, 2163. PDB ID.1N9V.

(11) Le, M. T.; Vanderheyden, P. M. L.; Szaszák, M.; Hunyady, L.; Kersemans, V.; Vauquelin, G. *Biochem. Pharm.* **2003**, *65*, 1329.

(12) Jorgensen, W. L.; Chandrasekhar, J.; Madura, J. D. *J. Chem. Phys.* **1983**, *79*, 926.

(13) AMBER 6, Case, D. A.; Pearlman, D. A.; Caldwell, J. W.; Cheatham, T. E., III; Ross, W. S.; Simmerling, C. L.; Darden, T. A.; Merz, K. M.; Stanton, R. V.; Cheng, A. L.; Vincent, J. J.; Crowley, M.; Tsui, V.; Radmer, R. J.; Duan, Y.; Pitera, J.; Massova, I.; Seibel, G. L.; Singh, U. C.; Weiner, P. K.; Kollman, P. A. University of California, San Francisco, 1999.

(14) Skaf, M. S. *J. Chem. Phys.* **1997**, *107*, 7996.

(15) Martínez, J. M.; Martínez, L. *J. Comput. Chem.* **2003**, *24*, 819. This program is available online at the following URL: http://www.ime.unicamp.br/∼martinez/packmol/index.html.

(16) Berendsen, H. J. C.; Postma, J. P. M.; Van Gunsteren, W. F.; DiNola, A.; Haak, J. R. *J. Chem. Phys.* **1984**, *81*, 3684.

(17) Cornell, W. D.; Cieplak, P.; Bayly, C. I.; Gould, I. R.; Merz, K. M.; Ferguson, D. M.; Spellmeyer, D. C.; Fox, T.; Caldwell, J. W.; Kollman, P. A. *J. Am. Chem. Soc.* **1995**, *117*, 5179.

(18) Kollman, P. A.; Dixon, R.; Cornell, W.; Fox, T.; Chipot, C.; Pohorille, A. In *Computer Simulations of Biomolecular Systems*; Wilkinson, A., Weiner, P., Van Gunsteren, W., Eds.; Elsevier: Amsterdam, 1997; Vol. 3, p 83.

(19) Gould, I. R.; Cornell, W. D.; Hillier, I. H. *J. Am. Chem. Soc.* **1994**, *116*, 9250.

(20) Van Gunsteren, W. F.; Berendsen, H. J. C. *Angew. Chem., Int. Ed. Engl.* **1990**, *29*, 992.

(21) Ryckaert, J. P.; Ciccoti, G.; Berendsen, H. J. C. *J. Comput. Phys.* **1977**, *23*, 327.

(22) Essmann, U.; Perera, L.; Berkowitz, M. L.; Darden, T.; Lee, H.; Pederson, L. G. *J. Chem. Phys.* **1995**, *103*, 8577.

(23) York, D. M.; Darden, T. A.; Pederson, L. G. *J. Chem. Phys.* **1993**, *99*, 8345.

(24) Humphrey, W.; Dalke, A.; Schulten, K. *J. Mol. Graphics* **1996**, *14*, 33. This program is available online at the following URL: http://www.ks.uiuc.edu/Research/vmd.

(25) Carpenter, K. A.; Wilkes, B. C.; Schiller, P. W. *Eur. J. Biochem.* **1998**, *251*, 448.

(26) Santos, E. L.; Pesquero, J. B.; Oliveira, L.; Paiva, A. C. M.; Costa-Neto, C. *Reg. Pept.* **2004**, *119*, 183.

(27) Correa, S. A. A.; Zalcberg, H.; Han, S. W.; Oliveira, L.; Costa-Neto, C. M.; Paiva, A. C. M.; Shimuta, S. I. *Reg. Pept.* **2002**, *106*, 33.

(28) Nikiforovich, G. V.; Marshall, G. R. *Biochem. Biophys. Res. Commun.* **2001**, *286*, 1204.

(29) D'Amelio, N.; Gaggeli, E.; Gaggeli, N.; Lozzi, L.; Neri, P.; Valensin, D.; Valesin, G. *Biopolymers* **2003**, *70*, 134.

(30) Tzakos, G. A.; Gerothanassis, P. I.; Troganis, A. *Curr. Top. Med. Chem.* **2004**, *4*, 431.

(31) Moutevelis-Minakakis, P.; Gianni, M.; Stougiannou, H.; Zoumpoulakis, P.; Zoga, A.; Vlahakos, A. D.; Iliodromitis, E.; Mavromoustakos, T. *Bioorg. Med. Chem. Lett.* **2003**, *13*, 1737.

(32) Fermandjian, S.; Fromageot, P.; Tistchenko, A. M.; Leicknam, J. P.; Lutz, M. *Eur. J. Biochem.* **1972**, *28*, 174.

(33) Fermandjian, S.; Sakarellos, C.; Piriou, F.; Juy, M.; Toma, F.; Thanh, H. L.; Lintner, K.; Khoslia, M. C.; Smeby, R. R.; Bumpus, F. M. *Biopolymers* **1983**, *22*, 227.